Aerodynamic Decelerator Systems Technology Conferences
30 Mar - 2 Apr 2015, Daytona Beach, FL
23rd AIAA Aerodynamic Decelerator Systems Technology Conference

10.2514/6.2015-2151

Parafoil Flight Mechanics: A Novel Flight Test Facility

Christiaan Redelinghuys[1], Steven Rhodes[2], Jordan L. Adams[2] *and* Tracy D. Booysen[3]
University of Cape Town, Cape Town, Western Province, 7701, South Africa

and

Arthur J. Grunwald[4]
Technion-Israel Institute of Technology, Haifa, 32000, Israel

With the objective of establishing a low-cost and rapid turn-around test capability for parafoil systems, a parafoil flight test facility, deemed novel, has been developed at the University of Cape Town. The uniqueness of the system resides mostly in the mobile launch system, the operational principle of which relies on synchronized canopy inflation and payload acceleration mechanisms. Various design considerations of the system are discussed. The helical spring energizing system is capable of launching a 30 kg payload at 14 m/s but the concept could be upgraded to launch larger vehicles. The airborne segment of the system consists of the parafoil canopy, its suspension and steering lines and a payload containing suitable reconfigurable avionics and actuators to allow the conduction of various types of experiments. Kinetic estimators mounted in the canopy and the payload allow motion reconstruction of the flight. Current research projects making use of the facility include inferring parafoil flight performance, the identification of aerodynamic stability derivatives and autopilot development. Initial system development and experimentation were conducted in a decommissioned quarry. It was found that the unique launching mechanism functions as intended and numerous faultless launches have been performed to date.

I. Introduction

Gliding parachutes, or parafoils, are currently widely used as human piloted devices as well as unmanned, autonomously guided aerial delivery systems. In both these applications, the aerodynamic performance of the parafoil system is of cardinal importance as it affects factors such as safety, stability, maneuverability, stand-off range, wind penetration capability and landing impact[1]. Autonomously guided systems rely on onboard avionics and servo actuators capable of providing navigation, guidance and control. System performance hence also strongly depends on the capabilities of these subsystems.

Synthesizing a new parafoil system usually relies on experience, theoretical analysis, simulation and flight testing. For a number of years, the development and testing of new parafoil systems has been taking place in many parts of the world, making use of a variety of techniques. Numerous mathematical models for parafoil aerodynamics and flight mechanics have seen the light, references 1 to 8 being typical examples, but generally testing has to support modeling. This is due to a number of simplifying assumptions normally implemented into simulation algorithms, such as assuming the canopy to be a rigid body, and uncertainty of aerodynamic parameters such as stability derivatives and apparent masses. Their flexible nature makes it cumbersome to test parafoil canopies in a wind tunnel, although it has been done[9]. Flight testing usually relies on launches from mountain tops, from fixed wing aircraft and helicopters. Canopy aerodynamic characterization has been performed by "flying" the canopy from the rear of a truck travelling along a runway[10]. Small parafoil systems have been studied by rolling take-offs using a wheeled propeller driven payload[11], manned micro-light releases, UAV releases[8] and balloon drops[12]. Low-cost testing of ejection seat parachutes has been achieved by means of a ground-based air-operated launcher[12].

[1]Professor, Department of Mechanical Engineering, Christiaan.redelinghuys@uct.ac.za, Senior Member
[2]Graduate student, Department of Mechanical Engineering
[3]Lecturer, Department of Mechanical Engineering
[4]Associate Professor, Department of Aerospace Engineering

Flight testing relying on launches from aircraft holds the advantage that the entire system, including both aerodynamics and control, is put to the test under realistic conditions. It has the drawback, however, that it is costly and the turn-around time from test to test is significant. Canopy aerodynamic testing from the back of a moving truck could provide much data at low cost, but this type of experimentation could not include testing of navigation and guidance systems. Balloon, micro-light and UAV drop tests are normally limited to small parafoil systems. Launches from mountain tops are very effective and widely used for developing human piloted systems. For unmanned systems, however, such launches would be restricted to low mass systems only.

In recent years, a unique parafoil system capability has been established at the University of Cape Town (UCT). The current approach is unique in that a mobile ground-based launching facility is used. The trailer-mounted launcher is capable of launching the parafoil system such that the canopy is fully inflated at launch, resulting in no altitude loss for inflation. Launching the instrumented parafoil system from a hilltop, or into a decommissioned quarry, allows various aspects of parafoil flight to be investigated. This includes aerodynamic parameter identification, design concept evaluation, optimization of glide slope and landing flare and guidance and control algorithm development. The payload onboard avionics and actuators are capable of performing navigation, guidance and control, and a ground-based pilot may fly the system remotely. An onboard kinematic estimator relying on IMU and GPS input provides trajectory data. Not having to rely on launching from a helicopter or an aircraft, implies huge cost savings and rapid turn-around time from test to test.

The present system is capable of launching a 30 kg payload at about 14 m/s. If it is to be used for the development of larger parafoil systems, scaling laws have to be applied to infer the aerodynamic characteristics of the full-scale prototype from the model testing, as is discussed below. In principle, the current design could be upgraded to handle larger systems.

This paper describes the functional characteristics of the UCT parafoil system and the main engineering considerations that were addressed during its development. The high-level system components to be discussed are the ground-based and the airborne segments, where the former includes the launcher and the ground-based flight control subsystem, and the latter includes the parafoil canopy and the payload, equipped with actuators and instrumentation. Suggested applications for the system are presented.

II. Mobile launch station

The main mechanical subsystem of the ground-based segment is the Mobile Launch Station (MLS). Mounted on a low-cost, lightweight trailer, the functionality of the launcher relies on a number of innovative concepts. Development of the MLS began with an extensive study of various launching concepts. Both trebuchet and spring powered catapult arm designs were demonstrated to be effective at performing repeatable launches of a small, one square meter parafoil into stable flights. In these designs, inflation of the canopy relies on a swing action effected by a rotating arm[14]. Once full confidence in the inflating concept had been gained, application of the concept towards the launch of larger parafoil and payload systems was investigated. For operational reasons it was desirable for the test vehicle to meet the standards for a model aircraft as defined by the South African Model Aircraft Association (SAMAA). The largest allowable vehicle mass and wingspan permitted are 25 kg and 6 m, respectively[15].

When the original launcher concepts were modelled to accommodate the larger parafoil and payload, it became clear that these would be unworkable. Launchers utilising only an arm to energise the larger payloads would be impractically long and would require large forces to accelerate. A linear launcher alone could provide the desired kinetic energy required for the payload, but linear launching was demonstrated to be very unpredictable for inflation of the canopy. In order to take advantage of each of the system types, a hybrid launcher was envisaged, which incorporated an arm for inflating the canopy and a linear launcher for accelerating the payload. By separating the rotational and linear components, the rotational catapult arm supports only the load on the parafoil. A T-bar was added at the end of the arm to support the parafoil across its span and assist in stable inflation.

A full scale demonstrator of the hybrid launcher concept was constructed to evaluate its performance. The demonstrator utilised widely available garage door springs for energizing both the linear launcher and the parafoil inflation arm. The advantages of a spring powered system included their relatively low cost and low weight (in comparison to pneumatic and counterweighted concepts). The system was tested with the same 6 m^2 parafoil which had been acquired for the flight testing program. Launch speeds in excess of 10 m/s could be achieved with a reduced payload of 20 kg.

Having successfully demonstrated the concept, work began on developing the operational launch system. The demonstrator had revealed three areas requiring specific attention: achieving the desired kinetic energy of the payload, safety of the launch operators during set up, and the mobility of the launching system.

The maximum payload was specified as 30 kg which was to be launched at 15 m/s. Experience with the prototype launcher indicated that approximately 50% of the spring energy was lost to friction and to the drag of the canopy during linear acceleration of the payload. Based on a 3 m linear track and including a reduction pulley system, it was calculated that a spring constant of 5 kN/m would be required for the linear launcher. For the arm, the extant pair of springs had been demonstrated as adequate for proper inflation of the canopy. Although a variety of spring arrangements incorporating custom made springs were investigated, low cost garage door springs were shown to be suitable for the task when arranged in four in-parallel sets of springs, each set consisting of two in-series springs. While the fully tensioned spring system could store sufficient potential energy to launch the larger payload, they posed a serious danger to personnel operating the launcher. For this reason, all aspects of the test flight were to be prepared without tension in the springs. The payload, trolley, parafoil and arm would, therefore, be placed in their pre-launch positions during set up with no tension in the springs. Once personnel were clear, a single remotely controlled winch would be used to energise the system and a 5 m long trigger line would be used to initiate launch.

The sequence shown in Fig. 1 describes the operation of the launcher. Initially the system is set up untensioned (i) allowing operators to perform checks on the readiness of the flight segment. When given the all-clear, the single tensioning winch is actuated and the system is ready for launch (ii). The launch operator waits for any wind gusts to subside before triggering the launch which releases the arm and inflates the canopy. When the canopy is fully inflated and is aligned vertically above the payload (iii) the arm contacts the deceleration cord which is connected to the payload trigger. The linear acceleration of the parafoil payload system then proceeds until the trolley crosses a pair of pulleys situated near the end of the launch rails (iv). From this point, the linear launcher springs begin to rebuild tension and pull back on the trolley. This action releases the payload from slots in the trolley and the launch is completed. A rigid arrestor line prevents overrun of the trolley.

With reference to Fig. 1i, the various components labelled on the figure are:

a) Payload
b) Swing arm
c) Trigger line
d) Payload anchor line
e) Arm deceleration cord
f) Winch
g) Arm spring set
h) Linear launcher spring set

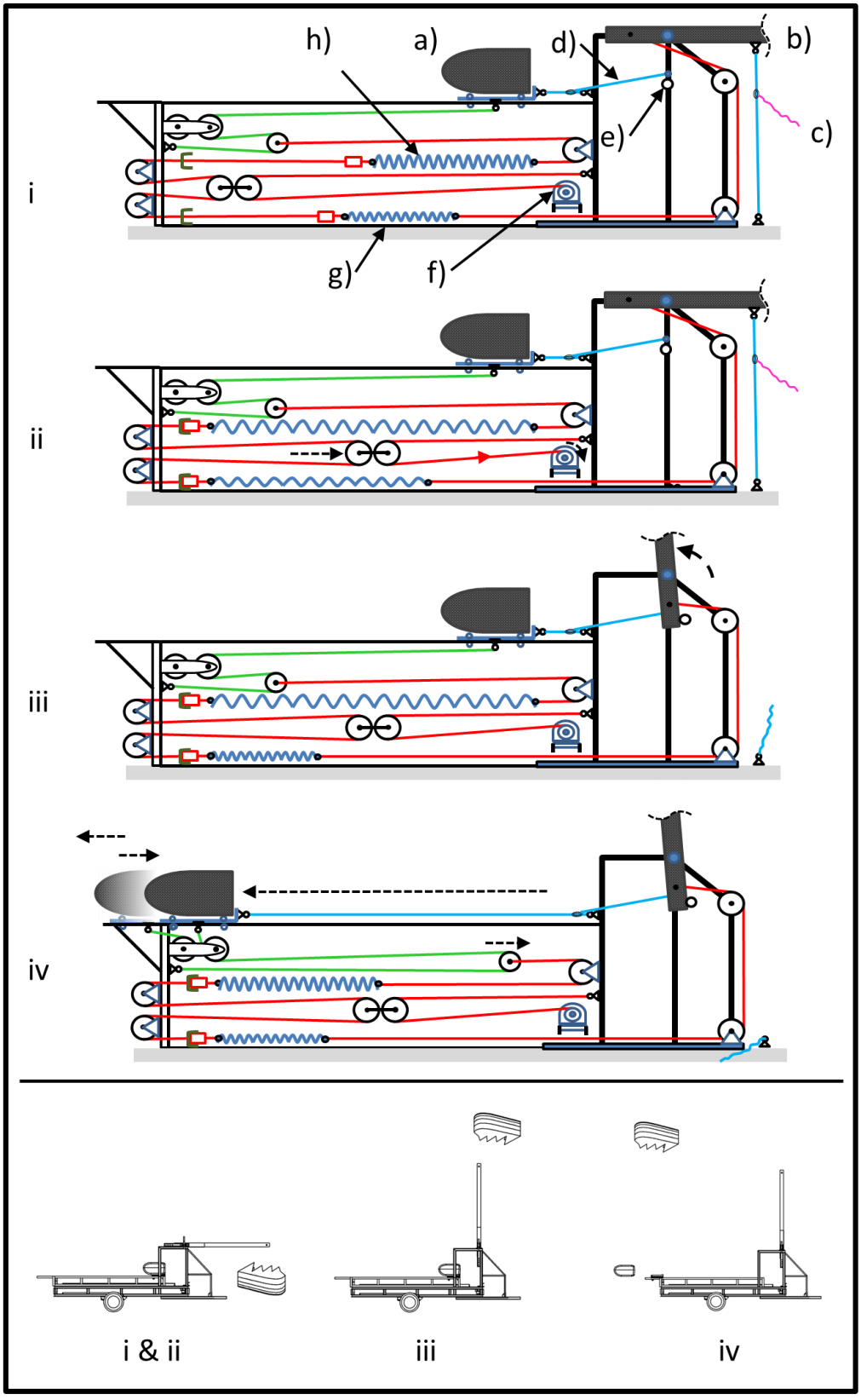

Figure 1. Operational sequences of the spring energising system

Having established a safe launch operational procedure with sufficient power, the mobility and functionality of the system was addressed through the final design phase for the system. As the parafoil-payload launch dimensions and launch station configuration approached design convergence, it became clear the mobile launch station would best be accommodated as a towed trailer.

The design for the trailer was perfected though several iterations before being constructed. The rotating arm for inflating the canopy was supported on a turret, with the pivot point located as close as possible to the payload. This minimizes the small loss in line tension due to a change in the line path length during the rotational phase of the launch. The parafoil lines are guided over secondary crossbars to keep them clear of all moving components. The length of the trailer allows the pretension in the springs to be adjusted to provide different launch energies and provides space for steel enclosures for all of the energising springs. The aluminium frame supporting linear launch rails from the demonstrator has been reused, but repositioned on the trailer to allow its full length to be utilised for acceleration. The rotating arm was redesigned using a lightweight carbon composite beam. This decreased the rotational inertia of the arm, allowing improved acceleration of the parafoil. The square section allowed for telescoping of the arm within its receiver. A composite T-bar slots into the rotational arm and cane be stowed during transport.

The completed MLS is capable of travelling over relatively rough terrain, increasing accessibility to launch sites accessible only via poorly maintained dirt roads. Preparation and assembly or disassembly can be completed in under an hour, while the design of the energising system facilitates quick turnaround times at reloading the system. Owing to the action of the launching mechanisms, no altitude is lost for canopy inflation as the airborne segment is launched into a stable glide from the initiation of the flight. This all increases the flexibility of the MLS in providing launch capabilities at the edges of steep descents for gliding parafoils, or from the ground in the case of powered parafoil systems.

Two suitable launch sites have been identified near UCT: For short duration flights, the first is a decommissioned stone quarry with maximum elevation around 90 m. This launch site is depicted in Fig. 2. The second site is a mountain pass with about 500 m elevation. The sites were chosen for their close proximity to the university research centre, good accessibility to launch and landing sites, inter-leading roads between launch and landing sites, low average wind speeds from April to September and low safety risk to the public. To date, the launcher has performed numerous successful parafoil launches.

Figure 2. A parafoil launch in process

III. Airborne Segment

The airborne segment consists of the parafoil canopy and its suspension and control lines and the payload comprising the composite outer shell, the steering box, the avionics and impact protection.

The parafoil canopy used for system testing is a 2/3 scale model of an aspect ratio 2.5 rectangular platform canopy, with a wing area of 13.66 m^2, that had been tested in the NASA Langley full scale wind tunnel [9]. This canopy has a

basic Clark Y airfoil section scaled up to a thickness of 21%. As the aerodynamic and stability and control characteristics of this canopy had been characterized in the Langley tests, it was considered a good choice for research on guided flight.

As discussed later, one of the objectives of the current system is to find the optimum trim angle for a particular parafoil configuration experimentally, with minimum effort. To ensure the canopy assumes the designed shape, each individual rigging line, from the parafoil to the confluence point, needs to be cut to the correct length. In the case of the 6 m^2 canopy used for commissioning the mobile launcher, there are 48 lines, with 24 unique line lengths. In order to minimise the number of unique lines made for varying trim angles and mean line lengths, a *trim frame* was designed to simplify the process, Fig. 3. The trim frame would be shaped to allow all successive lines in the chord-wise direction to be of the same length. Figure 3 below shows how the trim frame is shaped for the canopy, to allow the four chord-wise lines to be of equal length. This reduced the number of unique lines from 24 to just six – for each of the six span-wise locations of line groupings, on each half of the canopy. To adjust the trim angle and/or mean line length, only the two unique riser lines below each trim frame need to be adjusted for each configuration, compared with the original 24.

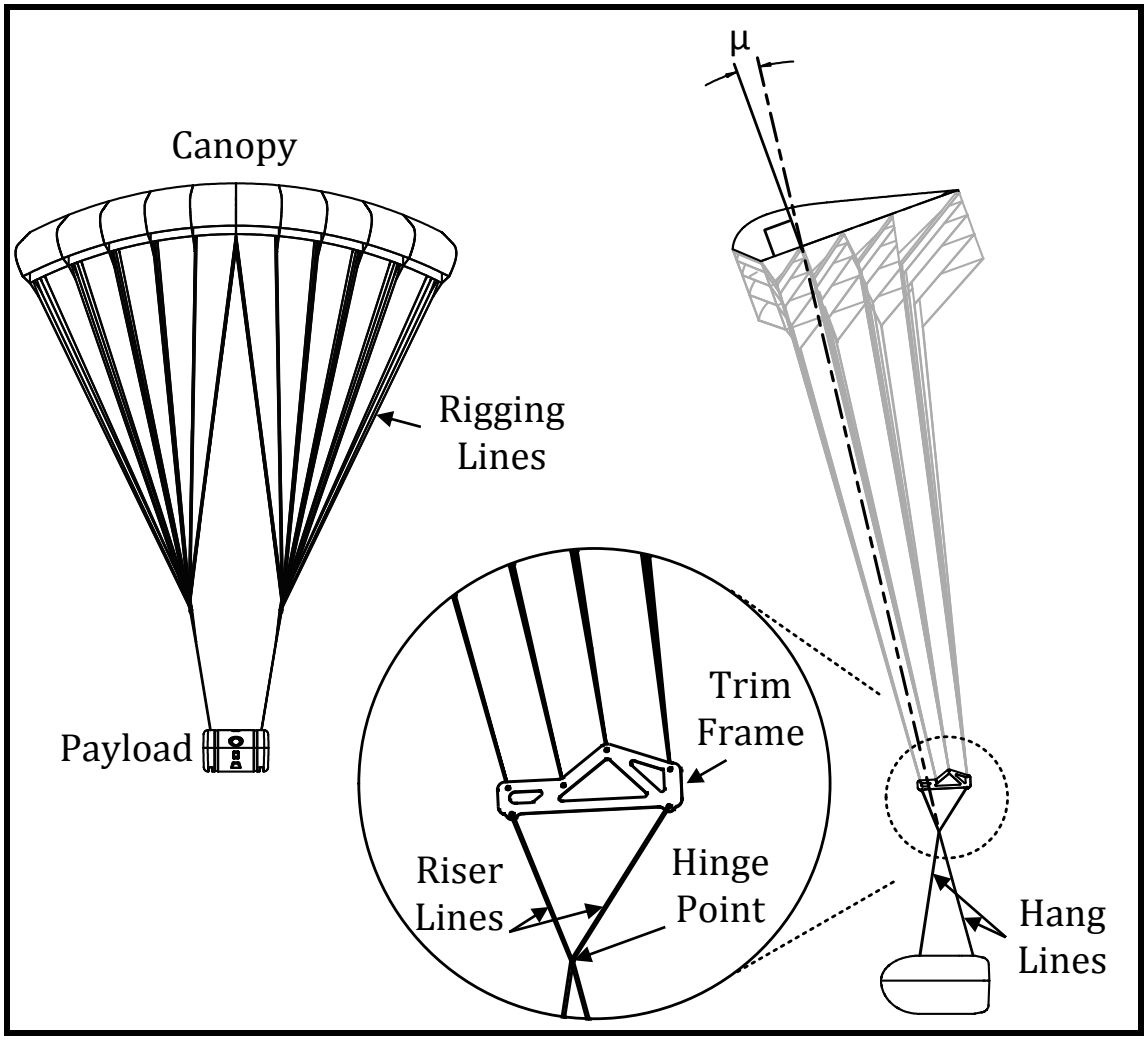

Figure 3. Trim frame and trim angle

A. Payload

The payload is comprised of a composite outer shell, a foam impact system, the controlling electronics, the camera and the winch system. The outer shell was moulded out of a combination of fibreglass, Kevlar and carbon fiber and provides a rugged box to house the more delicate subsystems. It was designed so that multiple outer shells could be

created. A particular shell was reusable for tests with gentle landings, but could be easily replaced if broken. The shell is split approximately halfway to improve accessibility and facilitate a vacuum moulded construction technique. It incorporates recesses for buttons, antennas, cables, cooling ports and camera mountings.

Two kinds of foam were shaped to provide support for the internal components. A closed cell polyethylene foam was used to form most of the supporting bulk owing to its relative rigidity and good shock absorbing properties. Two rectangular sections of open cell polyester foam were placed in front of the steering unit to allow more compliance, and hence reduce accelerations, in the event of a heavy frontal impact.

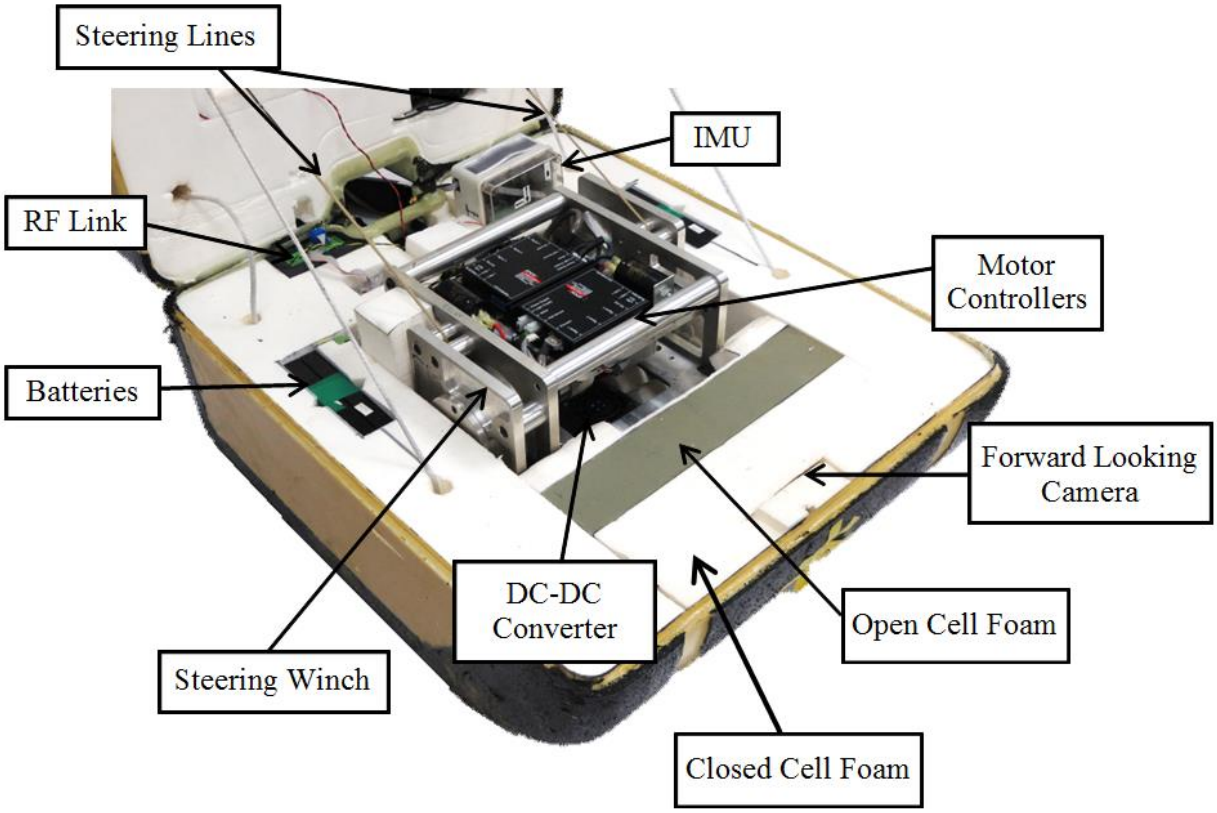

Figure 4. Physical lay-out of payload

Camera ports were included in the following directions: vertical up, vertical down and along the glide slope. These were sized to fit a GoPro Hero 2 camera with wireless backpack. The control lines pass through holes on the top shell and attach to the steering unit. The hang lines pass through to the bottom half of the payload and are fastened to brackets on the trolley-payload interface pins.

On the underside of the enclosure, the trolley-payload interface comprises of two longitudinal channels that form the main load bearing structure of the outer shell. A pair of vertically offset pins, in each channel, slide into slots in the launcher trolley. The slots constrain the payload in the vertical direction and only allow the payload to be released forwards as the trolley is decelerated. Figure 4 shows the physical lay-out of the on-board systems contained within the payload.

B. Parafoil control architecture overview

Figure 5 shows a schematic representation of the parafoil control architecture. Control of the airborne segment is effected by the steering box, housed within the payload, containing two DC motors with winch drums for actuating the canopy steering lines. As described later, these actuators were carefully chosen to a) allow harmonic steering inputs, for frequency response studies, and b) activate large amplitude brake deflections such as required during the landing flare.

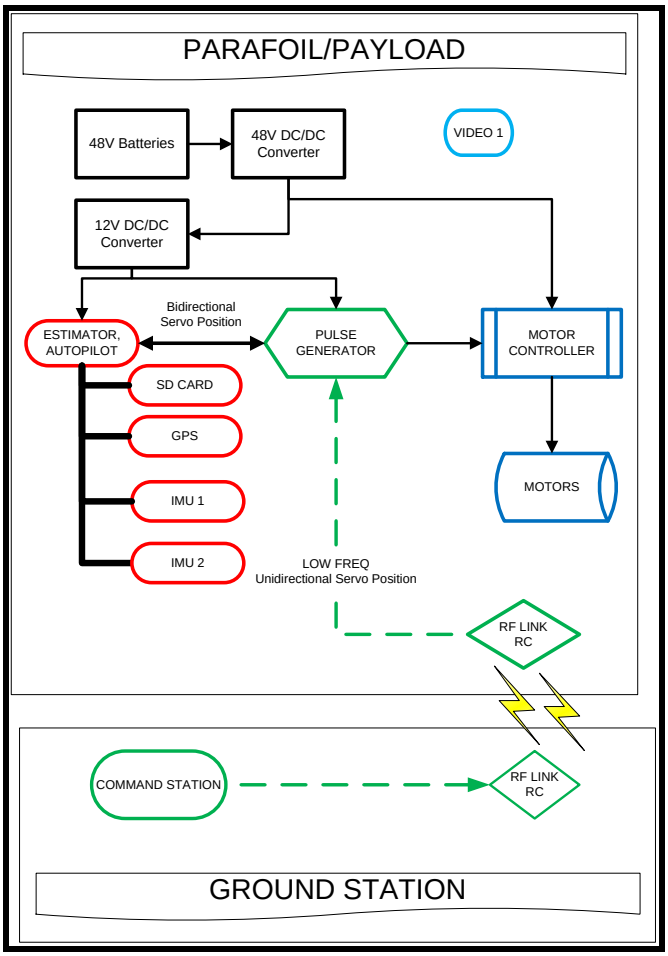

Figure 5. Parafoil control architecture

Power is supplied by means of four batteries which are regulated to 48V and 12V by two DC-DC converters. The EPOS motor controllers are connected to the bus voltage and in turn provide power to the motors. Since the steering line force increases with brake deflection, on the forward stroke the energy accumulated into the system will be drawn from the batteries and on the back-stroke part of this energy will be returned. Capacitors are used to buffer the changes in energy flow and to prevent large currents from being pushed back into the batteries. The motor controllers are configured in step/direction mode. Each pulse given to the EPOS controller results in a single position increment in the direction specified by the direction control pin input. The maximum acceleration, velocity and positional error is predefined and stored on the controller itself.

A pulse generator controller receives positional commands, compares the desired position with the current position and provides the pulses to the motors. These commands can be issued from the base station, an on-board autopilot or a manual system. During the initial setup of the steering box, the control lines need to be zeroed. This is done by using an external motor control keyboard. This keyboard monitors the battery voltages and moves the motors to the desired positions using an external plug. Once the keyboard is unplugged, the controller resets the current position as its zero position.

Two IMU's are used for measuring the system kinematics, one mounted in the payload and the other on the canopy. To securely locate an IMU on the canopy, a pocket and Velcro strap was sewn into the centre, leading-edge flare of the canopy. Directional stability in the relative wind is improved with a semi-rigid, lightweight backing plate sewn into the flare. A communication line connects the second IMU to the kinematic estimator in the payload. A kinematic estimator processes the IMU and GPS data, using a Kalman filter, to provide optimal trajectory and orientation measurement. The data from the two IMU's are logged on an SD card at 50 Hz and are also logged at the ground station at a reduced rate. After each flight, or series of flights, this data is downloaded and analysed.

Regarding control from the ground-based station, an interlink allows for switching between manual and autopilot flight, setting the gain of the full stick movement, going into flare mode and producing chirp signals (oscillatory inputs with gradually varying frequency). In ground control mode, the commands from the InterLink controller are processed, scaled and filtered by a ground based PC to produce the servo position commands. These commands are sent to the parafoil through InfinitQ 2.4 GHz RS-232 modems. For manual pilot control, the stick signals are filtered to prevent jerky and fast control stick motions to be imparted to the servos. The interlink allows for switching between manual and autopilot flight, setting the gain of the full stick movement, going into flare mode and producing chirp signals.

The ground station receives the vehicle states from the estimator Via a wireless communication link and, in turn, commands are be sent to the parafoil. The ground station could be used in various modes. It could either a) incorporate high-level guidance algorithms, b) issue open loop steering commands or c) be used for manual flight control. In addition, the ground station can display an interface depicting the parafoil position in space, its actual commanded flight path, the estimated wind directions and the intended touch-down site.

C. Specification of Winch Motors

Deflection of the canopy brakes is achieved by connecting each of the port and starboard steering lines to a drum that is rotated by an actuator via a gearbox. This actuation is capable of performing the following actions:

1. A very fast and short-stroke steering action; a sine wave of amplitude $A = 10$ cm at $f = 3$ Hz. This action is performed intermittently for short durations.
2. A medium fast steering action; a sine wave of amplitude $A = 30$ cm at $f = 1$ Hz. These actions could be performed continuously.
3. For the flare manoeuver, 80 cm to be travelled in 1 sec. The brake deflection rates for the flare are assumed to follow a trapezoidal profile against time.

In order to satisfy the speed and power requirements, two 150 W, 48 V DC, Maxon Brushless motors with matching planetary gear head with a 1:19 gear ratio are used. These motors are capable of performing the actions stated above as can be seen from Figs. 6 and 7 below, which show the demands of torque vs. motor speed for the various actions as well as the limits of motor operation. The torque demand for harmonic control line displacement at ω rad/s, is estimated by modeling this action as described below.

It is assumed that the brake line force is proportional to the line displacement, the constant of proportionality equaling K N/m. The steering line displacement, velocity and maximum power are calculated using the following equations:

$$s(t) = A \times (\sin(2\pi f t) + 1)$$
$$v(t) = A2\pi f \times \cos(2\pi f t)$$

From which it follows that

$$P_{max} = \pi f K A^2 \frac{3}{2}\sqrt{3}$$

With μ being the overall electrical and mechanical efficiency, the required maximum power is

$$P_{req} = P_{max}/\mu$$

Assuming 50% losses, the power requirements for the very fast, short stroke action, and the medium fast action are 30 W and 90 W, respectively. The trapezoidal flare manoeuver demands 100 W.

Using an effective motor, gearbox and drum moment of inertia of J and assuming that friction is a fraction $\mu_{friction}$ of the maximum line force in the opposite direction to the motion, the required drum torque is

$$T_{total} = T_{line\ force} + T_{acceleration} + T_{friction} = rKs(t) + \frac{J}{r}a(t) + \text{sign}(v)\mu_{friction} rKs_{max}$$

where $s(t) = \begin{cases} \{A(\sin(2\pi f t) + 1)) & \text{for harmonic motion or} \\ 0.5a_{flare}t^2 & \text{for the flare} \end{cases}$

and $a(t) = \begin{cases} -A(2\pi f)^2 \sin(2\pi f t) \text{ for harmonic motion or} \\ a_{flare} \text{ for the flare} \end{cases}$

and the motor torque is

$$T_{motor} = T_{total} / N\mu_{gear}$$

where μ_{gear} and N are the efficiency and transmission ratio of the planetary gear system, respectively. As can be seen from Fig. 6, the actuation system is capable of performing the medium fast oscillatory action continuously, but the very fast short stroke action can be performed only intermittently due to the rotational inertia of the rotating components. The flare manoeuver is within the capability of the actuator, as shown in Fig. 7.

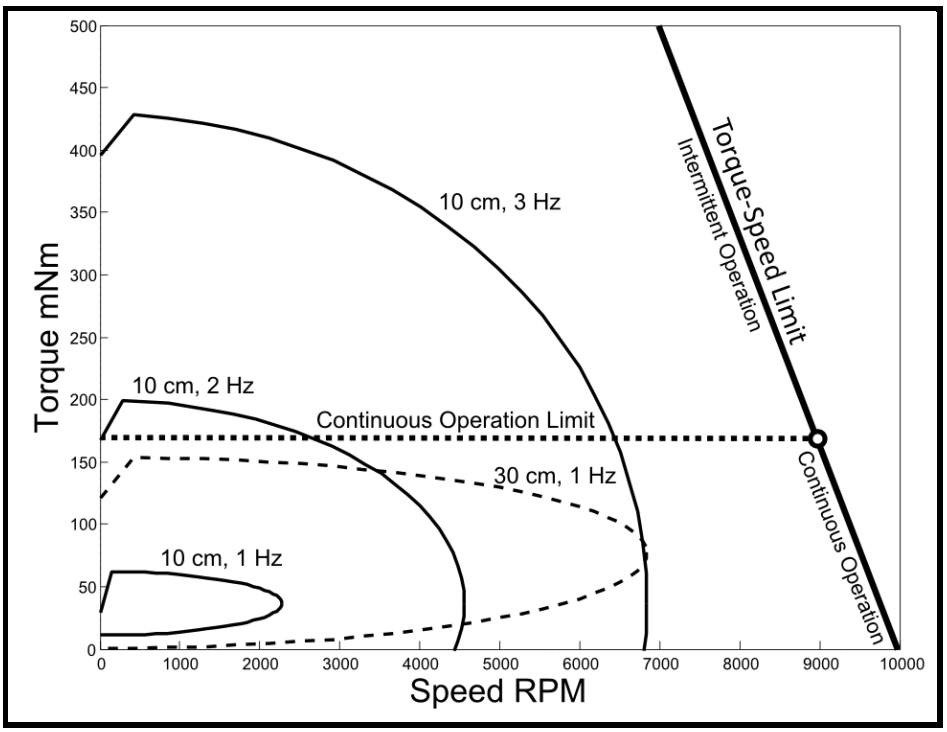

Figure 6. Motor torque versus speed curves for sinusoidal actuation

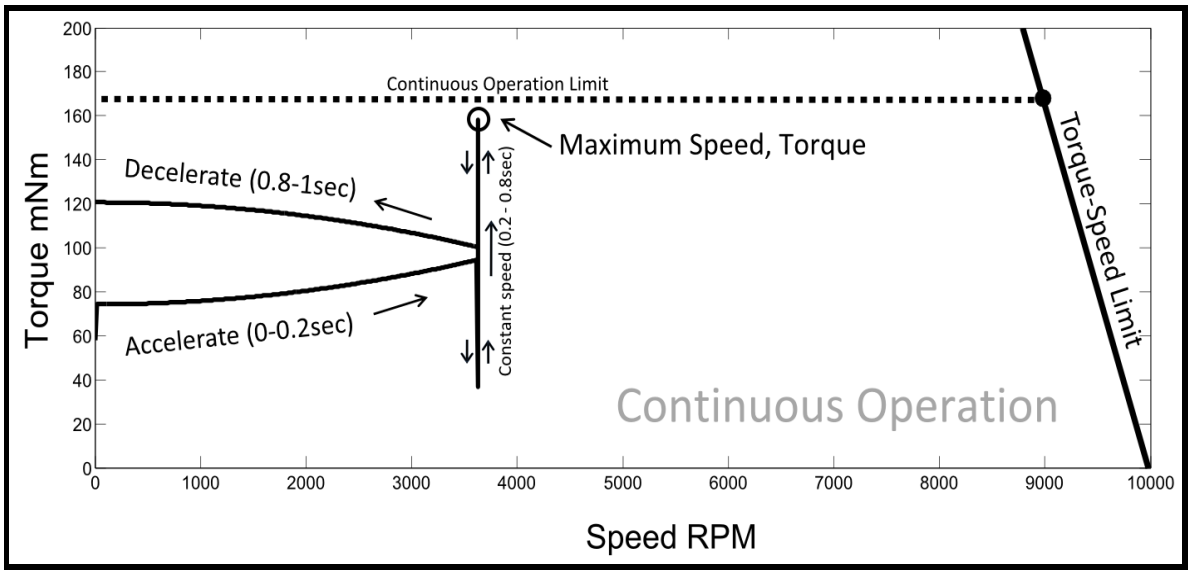

Figure 7. Motor torque versus speed for the flare manoeuver

IV. Capabilities of the test facility

The analysis of parafoil motions obtained from flight tests is often hampered by the presence of wind gusts and air turbulence. As one of the intentions of the current facility is the accurate experimental identification of vehicle flight performance, this type of testing is restricted to calm atmospheric conditions. Launch sites that offer adequate height and range, are accessible by light vehicles and have landing sites clear of obstacles are hard to find.

Post flight test data analysis is supported by an eight-degree-of-freedom flight simulation algorithm[16]. Depending on the specifics of the rigging geometry, the guidance sensor placement and the focus of the investigation, algorithms of fewer degrees-of-freedom may be used[8].

The parafoil testing facility as discussed above may be suited for the following applications although, admittedly, not all of these applications have as yet been put the test:

1. *Validation of design concepts:* Canopy design innovations are occasionally introduced, such as the control of glide slope using upper surface spoilers[17]. Due to the ability of the current system to impart actuator deflections and to infer the glide slope from flight tests, and the simplicity of the launcher logistics, the effectiveness of such innovations may be studied at low cost.

2. *The determination of glide-slope and lift-to-drag ratio:* As the vehicle flight state at launch does not normally agree with that of a steady glide, the trajectory exhibits an undesirable phugoid oscillation which dampens out as the vehicle glides further away from the launcher. As the damping ratio of the phugoid oscillation may be approximated by[18]

$$\zeta \simeq \frac{1}{\sqrt{2}L/D}$$

it follows that the phugoid oscillation of a high performance parafoil system will be more persistent than that of a high drag configuration. On the other hand, high L/D vehicles exhibit a shallower glide slope, and as the phugoid period is approximately

$$T = \sqrt{2}\pi\frac{V}{g}$$

it follows that high performance systems should be launched at low velocities and low wing loadings,

restricting the speed and shortening the phugoid period. The L/D ratio may be inferred from the phugoid damping ratio and also from the measured glide slope via the well-known equation $\tan(\gamma) = D/L$.

3. *The determination of optimal trim setting:* It is well known that a parafoil's gliding speed and L/D ratio depend on the trim angle. As discussed before, using a so-called trim frame, it is possible to very easily adjust the trim angle by just adjusting the line lengths to the confluence point. Initial experimentation clearly showed how the optimum glide slope could be determined within a short time period.

4. *Parameter identification of aerodynamic coefficients:* As the servos and avionics as discussed above are capable of imparting various types of control inputs such as ramp and oscillatory brake deflections, subsequent vehicle transients could be analyzed for the identification of aerodynamic stability derivatives.

5. *Optimization of the flare manoeuvre:* Studies have shown that landing point accuracy may be significantly improved by increasing the glide slope as the target area is approached[19]. An increase in glide angle invariably implies an increase in vertical velocity component, which in turn aggravates the landing impact. The payloads of parafoil delivery systems are usually protected against impact damage by designing them to be structurally sufficiently robust or using airbags to cushion the impact shock. Some fragile payloads might not lend themselves to being packaged in airbags in which case adequate sink rate reduction by means of a flare manoeuver is required. Parafoil recovery of a UAV, the latter not specially designed for hard impacts, is such an example. Different flare strategies may be efficiently studied with the current system, as short range flights in a quarry could be focused on the terminal flight phase.

6. *Autopilot development:* In a collaborative project with the nearby Stellenbosch University an autopilot has been developed for the parafoil system.

7. *Inference of large parafoil system flight characteristics:* The effect of parafoil scale on parameters such as turn rate and phugoid motion have been studied, e.g.[4,20]. The current facility is limited regarding the size of the parafoil system that could be launched. However, to a limited extent, larger systems may be launched at lower velocities. By means of dimensional analysis the performance of the model that is tested may be used to infer the uncontrolled characteristics of a larger prototype. The conditions that have to be satisfied to enable this inference are geometric similarity and the equality of the Reynolds number, and Froude number, relative density factors and the relative mass moment of inertia[21]. If the ratio of dimensions of the model to the prototype is λ, the required ratios between the model and prototype speeds and air kinematic viscosity are respectively given by

$$\frac{V_m}{V_p} = \sqrt{\lambda} \qquad \text{and} \qquad \frac{\nu_m}{\nu_p} = (\lambda)^{2/3}$$

As the air kinematic viscosity rises with altitude in the Standard Atmosphere, it follows that the characteristics of a scale model tested at sea level will correspond to those of the larger prototype flying at a higher altitude.

V. Conclusion

A parafoil launch and testing facility has been developed and commissioned at the University of Cape Town. To the authors' knowledge this apparatus is unique. The uniqueness of the system resides mostly in the mobile launch system, of which the operational concept relies on synchronized canopy inflating and payload acceleration mechanisms that allow fully inflated canopy launches. The helical spring energizing mechanism provides enough energy to launch a 30 kg payload at 14 m/s.

The system mobility and ease of deployment lends itself to various rapid and low-cost parafoil system development studies. Launching into a decommissioned quarry, for example, allows rapid turn-around time from test to test and comprehensive photographic monitoring of the entire flight. The onboard systems and ground station are reconfigurable, allowing control either by a human pilot or by an autopilot. In autopilot mode various actuator commands may be imparted, e.g. constant turn rate commands or ramp or oscillatory brake inputs. This enables the identification of parafoil aerodynamic stability derivatives and vehicle natural motions.

Various applications of the parafoil testing facility have been demonstrated. This includes a large number of faultless launches, the determination of optimum rigging trim setting and parafoil lift-to-drag ratio, the identification of phugoid period and damping, and human and autopilot control. Further projects are to be undertaken to further explore the facility's potential. This includes optimization of the flare manoeuver, comprehensive identification of aerodynamic parameters and navigation studies.

VI. Acknowledgments

This project was supported by the National Aerospace Centre of the University of the Witwatersrand, Johannesburg. The Electronic Systems Development Laboratory of Stellenbosch University provided inertial measurement units and an autopilot. Lafarge South Africa provided access to the decommissioned Dorstberg quarry near Cape Town.

References

[1]Lingard, J.S., "Ram-Air Parachute Design," Precision Aerial Delivery Seminar, 13th AIAA Aerodynamic Decelerator Systems Technology Conference, May 1995.

[2]Mortaloni, P.A., Yakimenko, O.A., Dobrokhodov, V.N., and Howard, R.M., "On the Development of a Six-Degree-of-Freedom Model of a Low-aspect ratio Parafoil Delivery System," AIAA Paper 2003-2105, 2003.

[3]Lissaman, P.B.S., and Brown, G.J., "Apparent Mass Effects on Parafoil Dynamics," AIAA Paper 93-1236, 1993.

[4]Brown, G.J. "Parafoil Steady Turn Response to Control Input," AIAA Paper 93-1241.

[5]Eslambolchi, A., and Johari, H., "Simulation of Flowfield around a Ram-Air Personnel Parachute Canopy," AIAA Paper 2013-1281, 2013.

[6]Mkrtchyan, H., and Johari, H., "Detailed Aerodynamic Analysis of Ram-Air Parachute Systems in Steady Flight," AIAA Paper 2011-2553, 2011.

[7]Toussaint, Cl., Cumer, Ch., Le Moing, Th., Poquillon, E., Coquet, Y., "Flight Dynamic Modelling of the PBO Parafoil using Sparse Preliminary Flight Test Data," AIAA Paper 2013-1386, 2013.

[8]Gorman, C. M., and Slegers, N. J., "Comparison and Analysis of Multi-body Parafoil Models with Varying Degrees of Freedom," AIAA Paper 2011-2615, 2011.

[9]Ware, G. M., and Hassell, J. L. Jr., "Wind-tunnel Investigation of Ram-air Inflated All-flexible Wings of Aspect Ratios 1.0 to 3.0," NASA TM SX-1923, December 1969.

[10]Brown, G. J., "Tethered Parafoil Test Technique," AIAA Paper A89-0903-CP, 1989.

[11] Gavrilovski, A., Ward, M., and Costello, M., "Parafoil Glide Slope Control Using Canopy Spoilers," AIAA Paper 2011-2517, 2011.

[12]Hiraki, K., Kawazoe, K., Imoto, T., and Inoue, M., "Balloon-Drop Test for Evaluation of Guiding Performance of Small-Parafoil Flight System," AIAA Paper 2007-2520, 2007.

[13]Downs, P. R., and Bartlett, R. P., "A Ground-based Air-operated Launcher for Parachute Testing," AIAA Paper A89-36024, 1989.

[14]Norton, W. A., "The Development, Optimisation and Testing of an Unmanned Parafoil Launch System," MSc(Eng) Dissertation, Department of Mechanical Engineering, University of Cape Town, August 2010.

[15]Anonymous, "Definition and Specification of Model Aircraft," Issue 2, The South African Model Aircraft Association (SAMAA), 2011.

[16]Redelinghuys, C., "A Flight Simulation Algorithm for a Parafoil Suspending an Air Vehicle," *Journal of Guidance, Control and Dynamics*, Vol. 30, No. 3, May-June 2007, pp. 791-803.

[17]Bergeron, K., Ward, M., Costello, M, and Tavan, S, "AccuGlide 100 and Bleed-Air Actuator Airdrop Testing," AIAA Paper 2013-1378, 2013.

[18]Ashley, H., *Engineering Analysis of Flight Vehicles*, Dover, Mineola, New York, 2012.

[19]Ward, M., and Costello, M., "Autonomous Control of Parafoils using Upper Surface Spoilers," AIAA Paper 2013-1379, 2013.

[20]Goodrick, T.F., "Scale Efffects on Performance of Ram Air Wings," AIAA Paper 84-0783, 1983.

[21]Wolowicz, C. H., Bowman, J. S. Jr., and Gilbert, W. P., "Similitude Requirements and Scaling Relationships as Applied to Model Testing," NASA TP 1435, August 1979.